HEFAT2012
9th International Conference on Heat Transfer, Fluid Mechanics and Thermodynamics
16 – 18 July 2012
Malta

OPTIMIZATION OF WASTE HEAT RECOVERY USING AN ORC IN A LARGE RETAIL COMPANY

Lecompte S.*, Huisseune H., De Schampheleire S., De Paepe M.
*Author for correspondence
Ghent University, Department of Flow, Heat and Combustion Mechanics,
Sint-Pietersnieuwstraat 41, 9000 Gent, Belgium
E-mail: Steven.Lecompte@UGent.be

ABSTRACT

Combined heat and power (CHP) systems are able to increase the total energy use of primary energy sources. In the CHP system studied in this paper internal combustion engines produce electricity and the hot engine cooling water is used for the heating of buildings. However, there is still waste heat left which can be fed to an organic Rankine cycle (ORC) to produce electricity. The objective of this study is to design an economic optimal ORC system taking into account the variable load for heating and the change in ambient temperature during a year. Also the auxiliary equipment such as pumps and fans are considered. A thermodynamic steady-state model is developed to simulate the changing behavior hour-by-hour of the complete system in different operating conditions. The ORC efficiency strongly varies over a year. The model allows selecting the optimal size of the heat exchangers (condenser and evaporator), the optimal mass flow rates and the maximal power of fans and pumps needed for the considered application.

INTRODUCTION

The world energy use has risen more than 40% between 1990 and 2008 [1]. Together with the growing demand, the energy prices keep on increasing. Furthermore, statistical studies show that low grade waste heat accounts for more than 50% of the total heat generated in the industry [2]. Therefore many companies are interested to exploit new technologies to make valuable use of low grade waste heat.

A possible solution is the use of low grade waste heat for the heating of buildings. The drawback is that in temperate climates the waste heat is unused during summer, while during winter it is possible that not all waste heat is used.

Organic Rankine cycles (ORC) offer the possibility to generate electricity from the left over waste heat even with temperatures below 100°C [3]. The choice for an ORC to convert the waste heat to power is influenced by the availability and simplicity of the technology and the research already done on the subject. In literature the selection of fluids for different working conditions is covered extensively by various authors (e.g. Wang et al. [4], Saleh et al. [5], Dai et al [6]).

NOMENCLATURE

CHP	Combined heat and power
LMTD	Logarithmic mean temperature difference
ORC	Organic Rankine Cycle
SIC	Specific investment cost
ICE	Internal combustion engine
TCC	Total component costs

Symbols

A	[m²]	Area
d	[m]	Diameter
k	[kW/m²K]	Heat transfer coefficient
L	[m]	Length
$\dot{m}$	[kg/s]	Mass flow rate
Q	[kW]	Heat
T	[°C]	Temperature
$\dot{V}$	[m³/s]	Volume flow rate
W	[kW]	Power

Greek symbols

η	[-]	Efficiency
ε	[-]	Isentropic efficiency

Subscripts

a	Air
af	After (in the direction of the mass flow)
amb	Ambient
bf	Before (in the direction of the mass flow)
c	Condensor
cond	Condensing
drop	Pressure drop
e	Evaporator
evap	Evaporating
h	Cooling circuit fluid
heating	Heating of buildings
in	Input
out	Output
r	Working fluid ORC
sat	Value at saturation point
sub	Subcooling
sup	Superheating

Quoilin et al. [7] investigated the optimisation potential by regulating the evaporation pressure in operation. A thermo-economic model was also developed [2]. They found that a thermodynamic optimization can differ significantly from a thermo-economic optimization. The optimal specific investment cost (SIC) for an ORC by using R245fa as working fluid was estimated at 2700 €/kWe. Schuster [3] made the assumption of a specific investment cost of 3755 €/kWe. Rettig et al. [8] compiled data of specific investment costs available from case studies and quotes from manufacturers. They showed that for ORC's below 500 kWe the SIC rapidly increases. At 500 kWe and 250 kWe the SIC is respectively around 2250 €/kWe and 3000 €/kWe.

The specific case used in this study is a combined heat and power (CHP) system driven by an internal combustion engine where waste heat is available from the closed loop engine cooling circuit. Nowadays, the waste heat is used for building heating and the rest is dumped to the atmosphere. The objective of this study is to investigate the feasibility of an ORC fed by the excess waste heat after building heating. The load on the ORC will vary significantly in winter because then more heat is needed for heating of the buildings. Ambient temperatures also vary strongly, which affects the condenser performance. First, an economic optimal ORC system was designed for a closed loop heat source from a well-chosen reference working point. Next, this design was used in an hour-by-hour quasi-steady state simulation over a reference year to get insight into the possible net energy production. The mass flow rates of the cooling circuit, the working fluid and the air to the condenser were regulated to achieve optimal cycle pressures in the ORC. To the authors' knowledge, these kind of quasi-steady state simulations have not yet been done.

The coming months, the Kriging optimization method [9] will be used for optimizing this initial reference design to an optimal design for a reference year.

SYSTEM DESCRIPTION AND ASSUMPTIONS

Data from a retail company that currently has a CHP system is used as a test case. Figure 1 shows the simplified setup. Waste heat Q_{ICE} is available from the closed cooling circuit of the internal combustion engines. This heat is normally used for heating the buildings. The heat Q_{ICE}-$Q_{heating}$ is imposed as heat input to the ORC's evaporator. A thermostatic valve keeps the water entering the ORC at 90°C. Table 1 summarizes the constant parameters in the setup.

Table 1 Constant setup parameters of the system

Parameter	Value
T_{hi}	90 [°C]
cooling circuit medium	water
condenser medium	air
Q_{ICE}	3452 [kW]
$Q_{heating}$	hour-by-hour profile

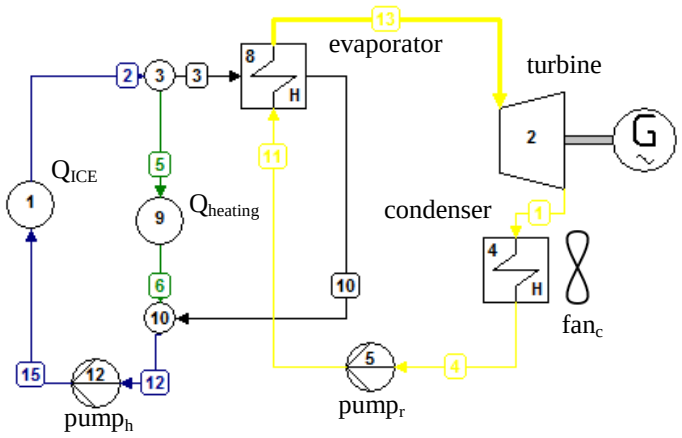

Figure 1 Simplified configuration of the CHP and ORC system

The fixed water inlet temperature of 90°C to the ORC implies that an increased evaporating pressure will result in an increased mass flow rate of the refrigerant. In other words, increasing the evaporating temperature with a constant mass flow rate will decrease the overall heat input. This effect can also be illustrated on the TS-diagram of the ORC in Figure 1. Decreasing the evaporator temperature will increase the glide slope between $T_{h,in}$ and $T_{h,out}$ and thus more heat can be valorised.

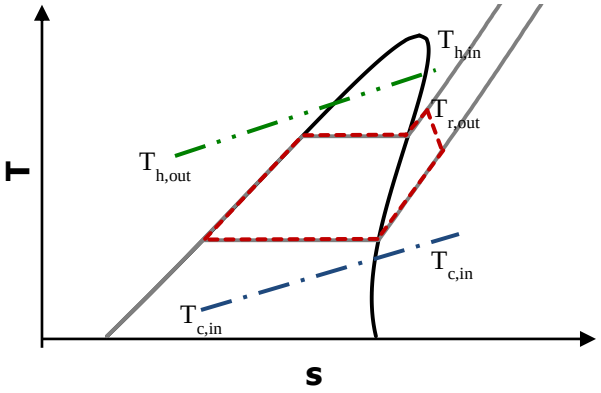

Figure 2 TS-diagram of the ORC

MODELLING

A steady state model of the ORC is made using MATLAB [10] in combination with the FluidProp library [11] for retrieving fluid properties.

Boundary conditions

The available waste heat and dry bulb temperature profiles of one year are read from a database and have a resolution of one hour. The dry-bulb temperatures from Brussels (Belgium) for a reference year are used. These are taken from Meteonorm [12] data included in TRNSYS 16 [13]. The power input profile Q_{in}, with a resolution of one hour is given by the retail company. The superheating of the working fluid after the evaporator is set at 5°C, the subcooling after the condenser is set at 3°C. R245fa is used as working fluid. According to Wang et al. [4], R245fa and R245ca are the most suitable working fluids for an engine waste heat application if safety levels and

environmental impacts are considered. R245fa also has a very broad application range: it is used as a foaming agent, as refrigerant and in ORC applications [3]. Table 2 summarizes the boundary conditions.

Table 2 List of boundary conditions

Parameter	Value
T_{amb}	dry bulb Meteonorm profile (Brussels)
T_{sup}	5 [°C]
T_{sub}	3 [°C]
Q_{in}	Q_{ICE}-$Q_{heating}$
Working fluid	R245fa

Evaporator and condenser

The evaporator is modelled using the logarithmic mean temperature difference (LMTD) method following a three-zone approach. This is illustrated in Figure 3.

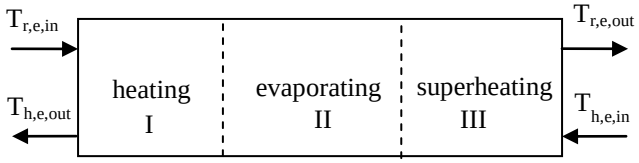

Figure 3 Model of evaporator following a three-zone approach

In the first zone the working fluid is heated to the evaporating temperature. The temperature of the cooling fluid is reduced with $\Delta T_{h,e,I}$.

$$\dot{m}_r \Delta h_{r,e,I} = \dot{m}_h c_{p,h} \Delta T_{h,e,I} = k_{e,I} A_{e,I} \Delta T_{LMTD,e,I} \quad (1)$$

$$\Delta h_{r,e,I} = \left(h_{r,e,in} - h_{r,e,evap}\right) \quad (2)$$

$$\Delta T_{h,e,I} = \left(T_{h,e,in} - T_{h,e,I}\right) \quad (3)$$

$$\Delta T_{LMTD,e,I} = \frac{(T_{h,e,out} - T_{r,e,in}) - (T_{h,e,I} - T_{r,e,evap})}{\ln \frac{T_{h,e,out} - T_{r,e,in}}{T_{h,e,I} - T_{r,e,evap}}} \quad (4)$$

In the second zone evaporation of the working fluid takes place. The temperature of the cooling fluid is further reduced with $\Delta T_{h,e,II}$.

$$\dot{m}_r \Delta h_{r,e,II} = \dot{m}_h c_{p,h} \Delta T_{h,e,II} = k_{e,II} A_{e,II} \Delta T_{LMTD,e,II} \quad (5)$$

$$\Delta h_{r,e,I} = \left(h_{r,e,evap} - h_{r,sat}\right) \quad (6)$$

$$\Delta T_{h,I} = \left(T_{h,e,I} - T_{h,e,II}\right) \quad (7)$$

$$\Delta T_{LMTD,I} = \frac{(T_{h,e,I} - T_{r,e,evap}) - (T_{h,e,II} - T_{r,e,evap})}{\ln \frac{T_{h,e,I} - T_{r,e,evap}}{T_{h,e,II} - T_{r,e,evap}}} \quad (8)$$

The third zone includes the superheating. The temperature of the cooling fluid is reduced with $\Delta T_{h,e,III}$.

$$\dot{m}_r \Delta h_{r,e,III} = \dot{m}_h c_{p,h} \Delta T_{h,e,III} = k_{e,III} A_{e,III} \Delta T_{LMTD,e,III} \quad (9)$$

$$\Delta h_{r,e,I} = \left(h_{r,e,sat} - h_{e,r,sup}\right) \quad (10)$$

$$\Delta T_{h,e,I} = \left(T_{h,e,II} - T_{h,e,III}\right) \quad (11)$$

$$\Delta T_{LMTD,I} = \frac{(T_{h,e,II} - T_{r,e,evap}) - (T_{h,e,in} - T_{r,e,sup})}{\ln \frac{T_{h,e,II} - T_{r,e,evap}}{T_{h,e,in} - T_{r,e,sup}}} \quad (12)$$

$$A_e = A_{e,I} + A_{e,II} + A_{e,III} \quad (13)$$

The mass flow rate of the working fluid is derived from the given heat input:

$$q_{in} = \dot{m}_r (h_{r,in} - h_{r,out}) \quad (14)$$

This results in 8 equations and 8 unknown variables ($A_{e,I}, A_{e,II}, A_{e,III}, T_{e,h,I}, T_{e,h,II}, T_{e,h,out}, \dot{m}_r, \dot{m}_h$). This system of nonlinear equations is numerically solved using the Trust-Region Dogleg Method [14].

The condenser model is analogue to the evaporator model, see Figure 4. The heat transfer coefficients [15] used in the evaporator and condenser are listed in Table 3.

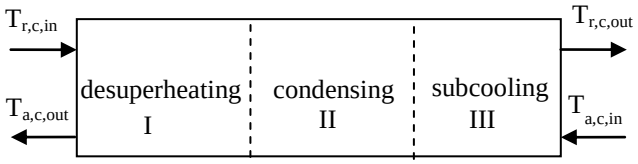

Figure 4 Model of condenser following a three-zone approach

Table 3 Used heat transfer coefficients [15]

Heat transfer coefficients	Value [kW/(m²K)]
$k_{e,I}$	0.5
$k_{e,II}$	1.2
$k_{e,III}$	0.2
$k_{c,I}$	0.2
$k_{c,II}$	0.5
$k_{c,III}$	0.5

Turbine, pumps and fans

The heating transfer fluid pump, the working fluid pump, the condenser fan and the ORC turbine are also incorporated in the model. They are all modelled by their isentropic efficiencies which are given in

Table 4.

$$\varepsilon_{pump|fan} = \frac{\Delta h_{s,pump|fan}}{\Delta h_{pump|fan}} = \frac{h_{s,af,pump|fan} - h_{bf,pump|fan}}{h_{af,pump|fan} - h_{bf,pump|fan}} \quad (15)$$

$$\varepsilon_{turbine} = \frac{\Delta h_{,turbine}}{\Delta h_{s,turbine}} = \frac{h_{af,turbine} - h_{bf,turbine}}{h_{s,af,pump|fan} - h_{bf,turbine}} \quad (16)$$

$$\dot{W}_{turbine} = \Delta h_{turbine} \quad (17)$$

$$\dot{W}_{pump|fan} = \Delta h_{pump|fan} \quad (18)$$

Table 4 List of isentropic efficiencies

Isentropic efficiency	Value [-]
$\varepsilon_{pump,h}$	0.60
$\varepsilon_{pump,r}$	0.60
ε_{fan}	0.60
$\varepsilon_{turbine}$	0.70

Cycle

The thermodynamic performance indicators used are the net cycle efficiency η_{net} and gross cycle efficiency η_{gross} and are defined as:

$$\dot{W}_{net} = \dot{W}_{turbine} - \dot{W}_{pump,h} - \dot{W}_{pump,r} - \dot{W}_{fan} \quad (19)$$

$$\eta_{net} = \frac{\dot{W}_{net}}{Q_{in}} \quad (20)$$

$$\eta_{gross} = \frac{\dot{W}_{turbine}}{Q_{in}} \quad (21)$$

Thermo-economic model

The thermodynamic model is further extended with the cost functions of the materials and equipment needed, which are summarized in Table 5. In the thermo-economic model the objective function for optimization is the specific investment cost (SIC) in €/kWe [2]:

$$SIC = \frac{Cost_{Labor} + Cost_{Components}}{\dot{W}_{net}} \quad (22)$$

The diameters of the pipings are calculated in the design phase by limiting the speed of the fluids in the ORC to 6 m/s and the airflow to 1 m/s. In total 10 m of piping is assumed.

Table 5 Component costs [2]

Component	Dependent variable	Cost [€]
Turbine	Volume flow rate [m³/s]	$1.5 \cdot (225 + 170 \cdot \dot{V}_{turb})$
Heat exchangers	Heat exchange area [m²]	$190 + 310 \cdot A$
Working fluid pump	Maximal power [kW]	$900 \cdot (\frac{\dot{W}_{pump}}{300})^{0.25}$
Cooling fluid pump	Maximal power [kW]	$500 \cdot (\frac{\dot{W}_{pump}}{300})^{0.25}$
Condenser fan	Maximal power [kW]	$100 \cdot (\frac{\dot{W}_{pump}}{300})^{0.25}$
Piping	Pipe diameter [mm]	$(0.89 + 0.21 \cdot d_{pipe}) \cdot L_{pipe}$
Control system	/	500
Miscellaneous hardware	/	300
Labour	Total component costs (€)	$0.3 \cdot TCC$

RESULTS AND DISCUSSION

The design procedure to develop a thermo-economic optimal design for a specific reference year consists of three steps. In the first step an optimized design for a fixed working point is made. Next, a quasi-steady state simulation is performed with this design to evaluate the mean net power production throughout a reference year. This mean net power production leads to a new estimate of the SIC. In the last step, variations in heat exchanger sizing, pumps and fans are made to search for an optimum SIC taking into account the varying operating conditions over a year. This will be done using the Kriging optimization method [9].

Reference design in fixed working point

A well-chosen fixed reference working point was selected to make a first design of the system. In summer the full load of 3452 kW is available for the ORC. It is thus preferable that the ORC can work in these conditions. The high ambient temperatures in summer lower the efficiency of the ORC and increase the heat exchanger size and thus the cost of the system. In winter the ambient temperatures are lower and therefore the net efficiency of the ORC will be higher. For the preliminary design an ambient temperature of 20°C was chosen. All the parameters of the design case are listed in Table 6.

It is assumed that the evaporator is designed in such a way that the pressure drop of the cooling fluid is limited to 1 bar [16] and the air-side pressure drop of the condenser is limited to 0.001 bar [17]. These pressure drops are defined for the design mass flow rates. All the parameters of the design case can be found in Table 6.

Table 6 Reference working point parameters

Parameter	Value
T_{amb}	20 [°C]
Q_{in}	3452 [kW]
$P_{drop,a}$	0.001 [bar]
$P_{drop,h}$	1 [bar]

In Table 7 the results of the thermo-economic optimization are shown. The variables A_{evap}, A_{cond}, $m_{h,nom}$, $m_{a,nom}$, $m_{c,nom}$ are the design variables and are kept fixed troughout a quasi-steady state simulation as explained in the next section.

Table 7 Optimal values at reference working point

Variable	Optimal value
A_{evap}	316.99 [m²]
A_{cond}	457.40 [m²]
T_{evap}	75.79 [°C]
T_{cond}	40.14 [°C]
$m_{h,max}$	97.62 [kg/s]
$m_{a,max}$	285.25 [kg/s]
$m_{c,max}$	16 [kg/s]
SIC	2134 [€/kW]

Figure 5 and Figure 6 show variations around the optimal design point. Figure 5a gives the mass flow rate and efficiency as function of the evaporator temperature for a fixed evaporator size. It is clear that there is an optimal mass flow rate to maximize the net efficiency. Higher evaporating pressures (or temperature) result in higher gross cycle efficiencies but leads to higher mass flow rates in the cooling circuit and thus the net efficiency will have a maximum.

The price of piping and pumps will increase with higher mass flow rates. Therefore the maximum evaporating pressure that can be reached is dependent on the investment costs. By increasing the evaporator heat exchanger size a higher evaporating temperature can be achieved with the same mass flow rate but now the price of the evaporator increases as shown in Figure 6a.

The optimal size of the condenser is found in a similar way and is show in Figure 5b and Figure 6b. Increasing the air flow over the condenser or increasing the size of the heat exchanger will decrease the saturation temperature and therefore increase the gross efficiency of the cycle. The price of the fan and heat exchanger will increase.

Important to notice is that the condenser and evaporator variables are coupled. Hence, the optimization must be done

with a multi variable optimization algorithm, like the simplex search method of Lagarias et al. [18].

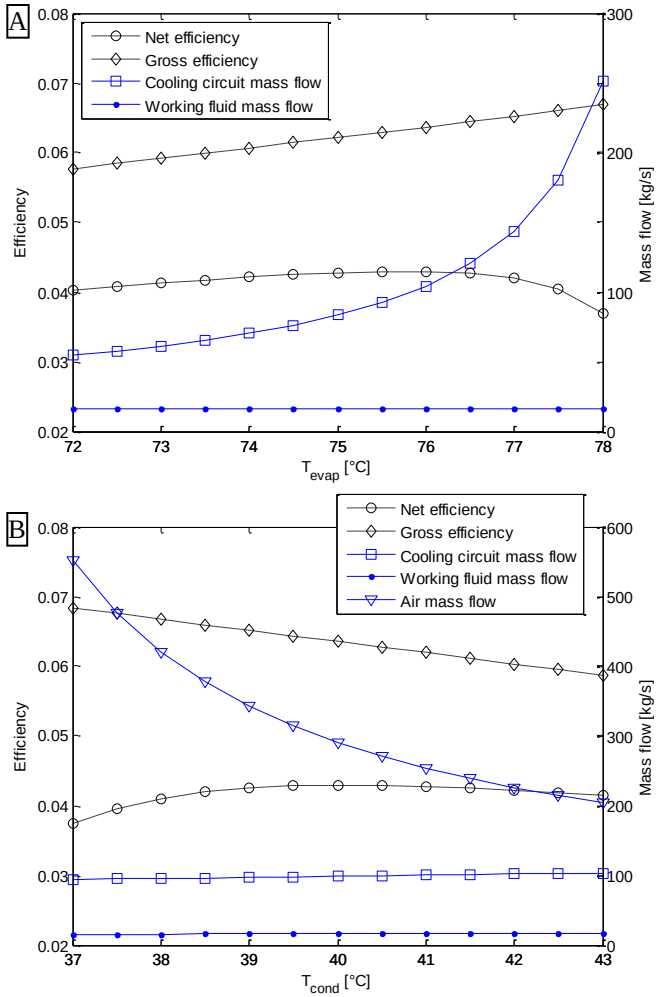

Figure 5 Sensitivity analysis mass flow rate
[Tamb = 20°C, Qin=3452 kW, Aevap=316.99 m², Acond=457.40 m²]
(a) Sensitivity evaporating temperature
(b) Sensitivity condensing temperature

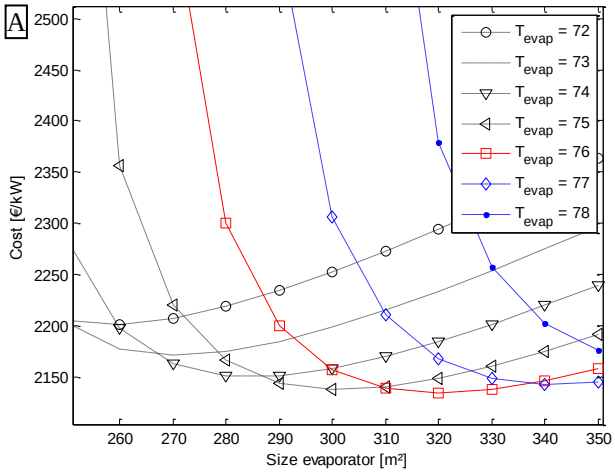

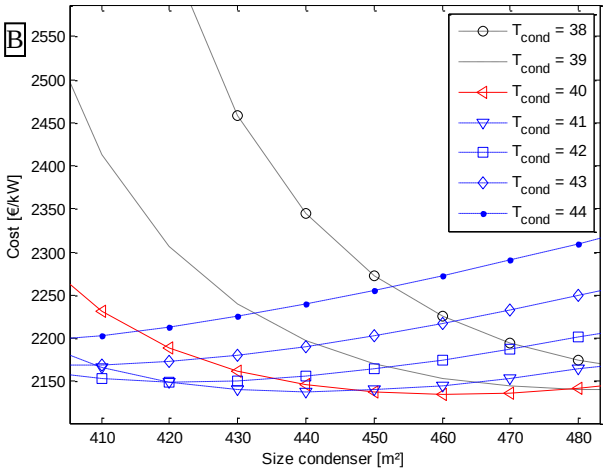

Figure 6 Thermo-economic optimization
(a) Size and evaporating temperature evaporator
[Tamb=20°C, Qin=3452 kW, Acond=457.40 m²]
(b) Size and condensing temperature condenser
[Tamb = 20°C, Qin=3452 kW, Aevap=316.99 m²]

Quasi-steady state simulation

In each working point, defined by the heat input Q_{in} and the ambient temperature T_{amb}, an optimal condensing and evaporating temperature exists corresponding to a maximum net efficiency. This is clear from Figure 6 and Figure 7. A map of the maximum net efficiencies in each working point (with the fixed design variables of Table 7) is shown in Figure 7. These maps can be made for different sets of design variables. The working region of the machine and the efficiency will change as shown in Figure 8 by way of illustration.

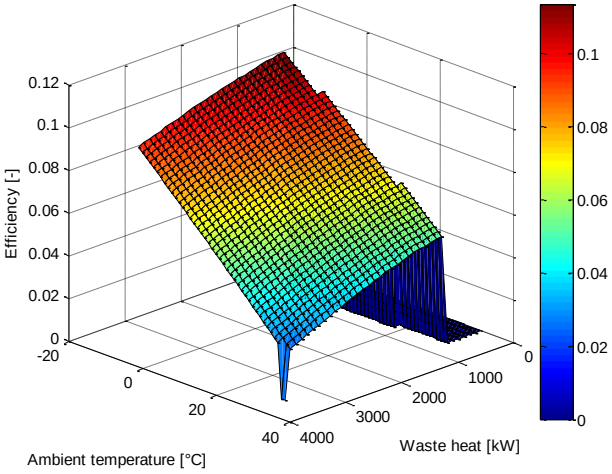

Figure 7 Net efficiency map [A_{evap}=316.99 m², A_{cond}=457.40 m², $m_{h,max}$=97.62 kg/s, $m_{a,max}$=285.25 kg/s, $m_{r,max}$=16 kg/s]

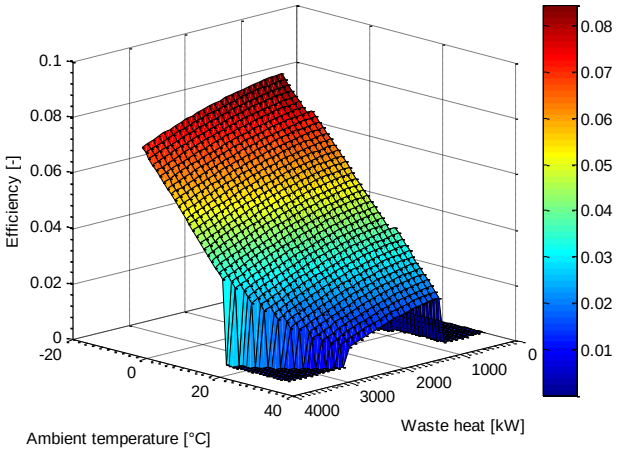

Figure 8 Net efficiency map [A_{evap}=200 m², A_{cond}=300 m², $m_{h,max}$=97.62 kg/s, $m_{a,max}$=285.25 kg/s, $m_{r,max}$=16 kg/s]

The design variables are then kept fixed throughout a year simulation and are used to calculate the cost of the pumps, fans and heat exchangers. The mean power output required to calculate the SIC is made by interpolating the data in the map according to the changing working conditions.

An extract of the resulting net efficiency and net output power is shown in Figure 9 and Figure 10, respectively. The efficiency varies with more than 0.3% and the net power output varies almost with 100 kW. The mean net efficiency, mean net power and SIC are shown in Table 8. The SIC has changed from the optimal value of 2134 €/kWe in the reference working point to 1518 €/kWe. This is because most of the time the ambient temperature is lower than 20°C. An optimal economic design must take this into account.

Table 8 Results quasi-steady state simulation

Variable	Value
Mean net efficiency	0.0619
Mean net power	209.9 [kW]
SIC	1518[€/kW]

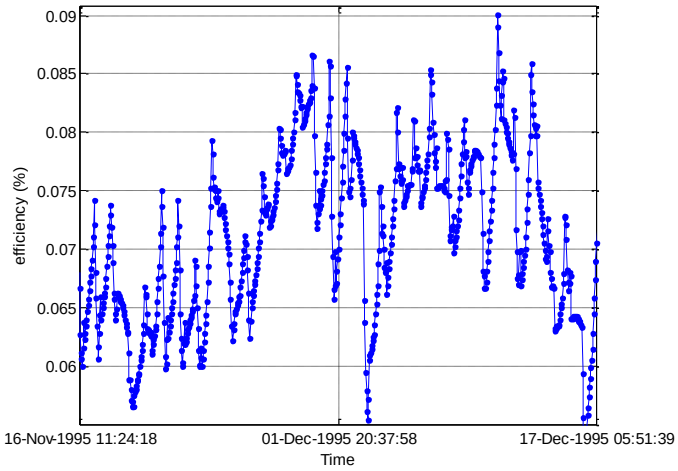

Figure 9 Quasi steady state simulation, net efficiency

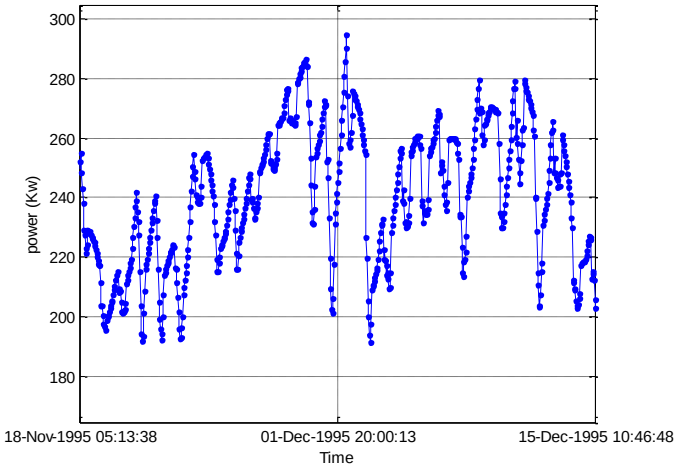

Figure 10 Quasi steady state simulation, net power output

Optimization of SIC in quasi-steady state simulation

By changing the design parameters the investment cost and the efficiency maps will change. Therefore an optimal design can be found for a specific year simulation. Quasi-steady state simulations will be performed for sets of different design variables. These sets are chosen with Latin Hypercube sampling. The Kriging optimization method [9] can then be used to search for an optimal set of design variables to minimize the SIC. This is the subject of future work.

CONCLUSION

The objective of this study was to make an economic optimal ORC by minimizing the SIC and by taking into account the changing ambient temperatures and heat input. In a fixed design it is necessary to change the mass flow rates of the ORC to maximize the net efficiency. The gross efficiency of the cycle keeps increasing with higher mass flow rates but the power needed from pumps and fans also increases.

Because of the strong variations in operating conditions (ambient temperature and heat input) a single reference design point does not give insight in the actual power output. The SIC changes from an optimal value of 2134 €/kW in the fixed reference working point to 1518 €/kW in the quasi-steady state simulation because of the higher net power output.

Analogue to the fixed reference working point, an optimal SIC exists in the quasi-steady state simulation. By considering different sets of design variables (A_{evap}, A_{cond}, $m_{h,max}$, $m_{a,max}$, $m_{r,max}$) with Latin Hypercube sampling and using the Kriging optimization this optimum can be found. This last part is a work in progress.

REFERENCES

[1] U.S. Energy Information Administration, *International Energy Outlook 2011*, 2011.

[2] Quoilin, S., Declaye, S., Tchanche, B.F., and Lemort V., Thermo-economic optimization of waste heat recovery Organic Rankine Cycles, *Applied Thermal Engineering*, Vol. 31, 2011, pp. 2885-2893

[3] Schuster, A., Karellas, S., Kakaras, E., and Spliethoff, H., Energetic and economic investigation of Organic Rankine Cycle

applications, *Applied Thermal Engineering*, Vol. 29, 2009, pp. 1809-1817
[4] Wang, E.H., Zhang, H.G., Fan, B.Y., Ouyang, M.G., Zhao, Y., and Mu, Q.H., Study of working fluid selection of organic Rankine cycle (ORC) for engine waste heat recovery, *Energy*, vol. 36, 2011, pp. 3406-3418.
[5] Saleh, B., Koglbauer G., Wendland, M., and Fischer, J., Working fluids for low temperature organic Rankine cycles, *Energy*, Vol. 32, 2007, pp. 1210-1221
[6] Dai, Y., Wang, J., and Lin, Gao., Parametric optimization and comparative study of organic Rankine cycle (ORC) for low grade waste heat recovery, *Energy Conversion and Management*, Vol. 50, 2009, pp. 576-582.
[7] Quoilin, S., Aumann, R., Grill, A., Schuster, A., Lemort, V., and Spliethoff, H., Dynamic modeling and optimal control strategy of waste heat recovery Organic Rankine Cycles, *Applied Energy*, Vol. 88, 2011, pp. 2183-2190.
[8] Rettig, A., Lagler, M., Lamare, T., Li, S., Mahadea, V., McCallion, S., and Chernushevich, J., Application of Organic Rankine Cycles (ORC), *World Engineers Convention*, Geneva, 4-9 September 2011.
[9] Forrester, A., Sobester, A., and Keane, A., Engineering Design via Surrogate Modelling: A Practical Guide, *Wiley*, July 2008.
[10] MATLAB version R2010a, *The Mathworks, Inc.*, 2010
[11] Colonna, P., and van der Stelt, T.P., *FluidProp 2.4: a program for the estimation of thermo physical properties of fluids*, Energy Technology section, Delft University of Technology, The Netherlands, 2004.
[12] Meteonorm, Global meteorological database for solar energy and applied meteorology, www.meteonorm.com
[13] Klein, S., TRNSYS-A Transient system simulation program, University of Wisconsin-Madison.
[14] Conn, N.R., Gould, N.I.M, and Toint, Ph.L., Trust-Region Methods, *MPS/SIAM Series on Optimization*, 2000.
[15] Sinnot, R.K., Towler, G., Chemical Engineering Design, *Elsevier*, Oxford, 2009, pp.821.
[16] James, RC., Chemical Process Equipment: Selection and Design, *Elsevier*, Oxford, 2005, pp.179.
[17] Lytron, Selecting a heat exchanger, Application Notes, 2012.
[18] Lagarias, J.C., Reeds, J.A., Wright, M.H., and Wright, P.E., Convergence Properties of the Nelder-Mead Simplex Method in Low Dimensions, SIAM Journal of Optimization, Vol. 9, 1998, pp. 112-147.